# Realization of NIST Luminous Flux Scale Using an Integrating Sphere with an External Source

Y. Ohno

ABSTRACT

An alternative method for realizing a luminous flux scale has been developed using an integrating sphere with an opening and an external source. The total flux from a lamp inside the sphere is calibrated against the known amount of flux introduced into the sphere from the external source through a limiting aperture. Corrections are made for the spatial nonuniformity and the incident angle dependence of the sphere response, and the spectral mismatch of the integrating sphere system. Theoretical analysis has been conducted by computer simulation. Using this method, a new NIST luminous flux scale has been realized with a relative expanded uncertainty (*k*=2) of 0.5 %.

ZUSAMMENFASSUNG

In einem alternativen Verfahren zur Realisierung einer Lichtstrom-Skala wird der Gesamt-Lichtstrom einer Lichtquelle im Inneren einer Ulbricht'schen Kugel mit dem in die Kugel eingeführten Lichtstrom einer äusseren Lichtquelle verglichen. Korrecturen werden angebracht für die räumliche Ungleichförmigkeit der Kugel, die Abhängigkeit der Kugel-Empfindlichkeit vom Einfallswinkel und den spektralen Empfindlichkeits-Unterschied des Kugel-Photometers. Theoretischen Untersuchungen mit Computer-Simulierung wurden unternommen. Mit diesem Verfahren wurde eine neue NIST Lichtstrom-Skala mit einer Unsicherheit von 0.5% (*k*=2) entwickelt.

RESUME

La réalisation d'une échelle de flux lumineux par une autre méthode a été développée en metant en oeuvre une sphère d'intégration munie d'une ouverture et une source extérieure. Le flux total émis par une lampe placée à l'intérieur de la shphère est déterminé par comparaison à un flux counu introduit dans la sphère, à partir de la source extérieure, par l'ouverture de dimension déterminée. Des corrections sont faites pour tenir compte de la non uniformité spatiale et de la depéndance angulaire de la résponse de la sphère, ainsi que de l'écart d'adaptation spectrale de la sphère d'intégration et du système associé. Des analyses théoriques ont été simulées par ordinateur. En utilisant cette méthode, une nouvelle échelle de flux lumineux du NIST a été réalisée avec une incertitude étendue (*k*=2) de 0,5 %.

KEYWORDS: Detectors, Luminous flux, Photometers, Photometry, Spectral response

## 1. INTRODUCTION

Traditionally, the luminous flux scale is realized using goniophotometers (goniophotometric method). It is often difficult, however, to build and maintain high-accuracy goniophotometers which require a large dark room and costly high-precision positioning mechanisms. Measurements are time consuming, resulting in longer burning time of lamps. Care must be taken to reduce sources of errors such as stray light, shadowing by lamp holders, data acquisition intervals and timing, etc.

To alleviate these difficulties, an alternative method for realizing a total luminous flux scale has been developed at NIST. This method (hereafter called the integrating sphere method) uses an integrating sphere with an opening, a limiting aperture, and an external source. The total flux of a lamp inside the sphere is calibrated against the known amount of flux coming into the sphere from the external source through the aperture. The incoming luminous flux is determined by the average illuminance at the aperture plane and the area of the aperture.

The integrating sphere method has an advantage in that a conventional integrating sphere can be used with small modifications, and the sphere can still be used for ordinary substitution measurements. Measurements are accomplished faster, resulting in shorter burning time of the lamps.

Corrections are needed for the spatial nonuniformity and the incident angle dependence of the sphere response and the spectral mismatch of the integrating sphere system. Theoretical analysis has been conducted by computer simulation. This method has been applied to experiments using a 2 m integrating sphere to realize the new NIST luminous flux scale.

## 2. BASIC CONCEPT

Figure 1 shows a diagram of an integrating sphere designed for this purpose. The luminous flux $\Phi_e$ (lm) from the external source introduced into the sphere is given by

$$\Phi_e = E_a \; S \tag{1}$$

where $E_a$ is the average illuminance (lx) over the limiting aperture of known area $S$. The sphere responsivity $R_s$ is calibrated by measuring the external source,

$$R_s = y_e \, / \, \Phi_e \tag{2}$$

where $y_e$ is the detector signal for the external source. With the external source turned off and the internal source turned on, and assuming the integrating sphere had a perfectly uniform spatial response, the total luminous flux $\Phi_i$ of the internal source would be obtained simply by

$$\Phi_i = y_i \; / \; R_s \tag{3}$$

where $y_i$ is the detector signal for the internal source. A self-absorption correction is not necessary if the internal source to be calibrated remains in the sphere when the external source is measured.

Two baffles are used to shield the detector and the opening from direct illumination by the internal source. The detector is exposed to the first reflection of the introduced flux from the external source in order to equalize the sphere responsivity for the internal source and that for the external source.

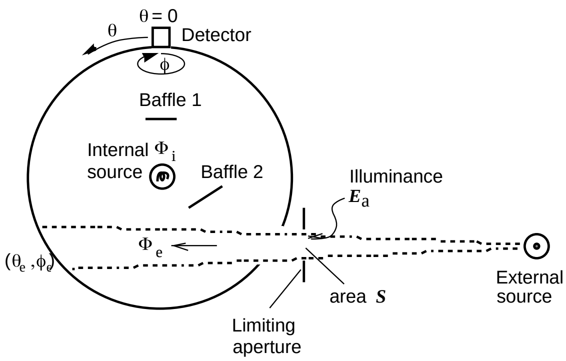


Figure 1 – Geometry of the simulation model

The baffles, however, cause spatial nonuniformities of the sphere response (detector signal divided by luminous flux). A systematic error is expected due to the nonequivalence of the sphere response between the conditions for the internal source and for the external source. To analyze the sphere characteristics and to find the optimum geometry of the sphere for this purpose, a computer simulation program was developed based on a flux tracing technique. Simulations were conducted for various arrangements of the opening, baffles, and the internal source with varied reflectance of the sphere wall. The simulation predicted an equivalence (within 0.1 %) of the sphere response calculated for the design shown in Figure 1 [1].

## 3. PRELIMINARY EXPERIMENTS

To verify the results of the simulation, a prototype integrating sphere of the design shown in Figure 1 was built. The sphere (50 cm diameter, 98% wall reflectance) has an opening of 8.8 cm diameter and two baffles. A 1000 W quartz halogen lamp was placed at 50 cm from the limiting aperture (56 mm in diameter). Measurements were made with different sizes, locations, and angles of the baffles. The measurement results in the effect of baffle locations and angles were in good agreement with the simulation results.

The total luminous fluxes of four miniature lamps were measured using a small goniophotometer that was calibrated with the same 1000 W halogen lamp, and compared with the sphere measurements. It was found that a correction factor for the spatial nonuniformity of the sphere response should be experimentally determined since the performance of an actual integrating sphere is affected by uneven contamination of the coating and gaps between the two hemispheres, etc. With the spatial nonuniformity correction (described in 4. 1) applied, the luminous flux values measured with the two methods agreed to within 0.5 % [2].

## 4. CORRECTION TECHNIQUES

### 4.1 Spatial nonuniformity of the sphere response

The response of the integrating sphere is not uniform over the sphere wall. The spatial response distribution function (SRDF) $K(\theta, \phi)$ of the sphere is defined as the sphere response at a point $(\theta, \phi)$ of the sphere wall or on a baffle surface divided by the sphere response at (0, 0). (See Figure 1 for the definition of $\theta$ and $\phi$.) $K(\theta, \phi)$ can be obtained by measuring the detector signals while rotating a narrow beam inside the sphere. $K(\theta, \phi)$ is then normalized for the sphere response to an isotropic point source. The normalized SRDF, $K^*(\theta, \phi)$, is defined as

$$K^*(\theta, \phi) = 4\pi K(\theta, \phi) \Big/ \int_{\phi=0}^{2\pi} \int_{\theta=0}^{\pi} K(\theta, \phi) \sin\theta \, d\theta \, d\phi \qquad (4)$$

Using $K^*(\theta, \phi)$, the spatial correction factor $scf_e$ for the external source with respect to an isotropic point source is given by

$$scf_e = 1 / K^*(\theta_e, \phi_e) \qquad (5)$$

The spatial correction factor $scf_i$ for the internal source with respect to an isotropic point source is given by

$$scf_i = 1 \Big/ \int_{\phi=0}^{2\pi} \int_{\theta=0}^{\pi} I^*_{rel}(\theta, \phi) K^*(\theta, \phi) \sin\theta \, d\theta \, d\phi \qquad (6)$$

where $I^*_{rel}(\theta, \phi)$ is the normalized luminous intensity distribution of the internal source given by

$$I^*_{rel}(\theta, \phi) = I_{rel}(\theta, \phi) \Big/ \int_{\phi=0}^{2\pi} \int_{\theta=0}^{\pi} I_{rel}(\theta, \phi) \sin\theta \, d\theta \, d\phi \qquad (7)$$

where $I_{rel}(\theta, \phi)$ is the relative luminous intensity distribution of the internal source. $I^*_{rel}(\theta, \phi)$ is normalized so that its total luminous flux becomes 1 lm. Goniophotometry is necessary to measure $I_{rel}(\theta, \phi)$, but corrections for $scf_i$ (using goniophotometric data) are not necessary if the internal sources have uniform spatial distributions.

### 4.2 Incident angle dependence of the sphere response

The SRDF is defined for normal incidence to the sphere wall. The light from the external source is incident at 45°. When the incident angle is different, the diffuse reflectance of the sphere coating changes [3], which affects the sphere response. The incident angle dependence correction factor $\beta$ is obtained by

$$\beta = y_0 / y_{45} \qquad (8)$$

where $y_0$ is the detector signal when a stable beam source is placed in the center of the sphere irradiating the sphere wall at $(\theta_e, \phi_e)$ at 0° incidence, and $y_{45}$ is the detector signal when the source is placed on the optical axis of the external source irradiating the same part of the sphere wall at 45° incidence.

### 4.3 Spectral mismatch of the integrating sphere system

The spectral power distribution of the internal source may be different from that of the external source, and a spectral mismatch correction is needed. The spectral mismatch correction factor $ccf^*_i$ of the internal source against the Illuminant A (2856 K Planckian source) is given by

$$ccf^*_i = \frac{\int_\lambda S_A(\lambda) R_s(\lambda) \, d\lambda \int_\lambda S_i(\lambda) V(\lambda) d\lambda}{\int_\lambda S_A(\lambda) V(\lambda) \, d\lambda \int_\lambda S_i(\lambda) R_s(\lambda) d\lambda} \qquad (9)$$

where $S_i(\lambda)$ is the relative spectral power distribution of the internal source, $S_A(\lambda)$ is that of the Illuminant A, and $R_s(\lambda)$ is the relative spectral responsivity of the integrating sphere system. $R_s(\lambda)$ can be obtained by measuring the relative spectral responsivity of the detector $R_d(\lambda)$, and the relative spectral throughput of the integrating sphere $T_s(\lambda)$ as

$$R_s(\lambda) = R_d(\lambda) \, T_s(\lambda) \qquad (10)$$

The spectral mismatch correction factor $ccf^*_e$ of the external source against the Illuminant A is given by Eq.(9) with $S_i(\lambda)$ replaced by the relative spectral power distribution $S_e(\lambda)$ of the external source.

## 5. REALIZATION OF THE NIST LUMINOUS FLUX SCALE

### 5.1 Experimental set-up

Figure 2 shows the geometry of the modified NIST 2 m integrating sphere used in this work. The sphere is coated with barium sulfate paint with a reflectance of 96 % to 98 % in the visible region.

An opening of 10 cm in diameter was cut at a position 45° away from the detector. The geometry was modified from the original design (Figure 1) for convenience of installing the external source. The portion illuminated by the external source is located in the same geometry (135° from the detector). Baffle 1 (20 cm in diameter) is located at 50 cm from the sphere center. Baffle 2 (15 cm in diameter) is located at 60 cm from the sphere center.

The detector is a $V(\lambda)$-corrected photometer with an opal diffuser (20 mm diameter) attached in front. It has a built-in transimpedance amplifier with gain settings from $10^4$ to $10^{10}$ V/A calibrated at each range (except $10^{10}$ range) with an uncertainty[†] of 0.02 %.

A built-in temperature sensor allows corrections for the photometer temperature drift. The linearity of the detector was measured to be constant over a flux range of $10^{-1}$ lm to $10^5$ lm to within 0.05 %.

A 1000 W frosted FEL type quartz halogen lamp operated at 2856 K was used as the external source. The lamp is placed at 70 cm from the limiting aperture, introducing a flux of ~2.7 lm through the 40 mm aperture.

Two stainless steel limiting apertures of 40 mm and 50 mm diameter, and 3 mm thick, are used. The area of the apertures was determined by the NIST Fabrication Technology Division with an uncertainty of 0.03%. The aperture is placed as close to the opening as possible to minimize diffraction losses.

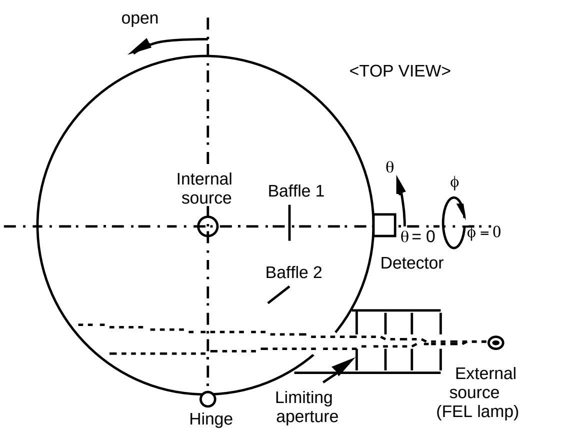


Figure 2 – Geometry of the modified NIST 2 m integrating sphere.

## 5.2 Correction measurements

The SRDF $K(\theta,\phi)$ was measured by rotating a beam source which was burning position insensitive. The source consists of a 6 V/1.2 W vacuum incandescent lamp equipped with a reflector (40 mm diameter) and a cylindrical hood (100 mm long). The inside of the hood is painted black, and the outside is painted white. The beam angle is ~10°. The SRDF measurements were made at 5° intervals for $\theta$ and 30° intervals for $\phi$. Figure 3 shows the SRDF $K^*(\theta, \phi)$ of the integrating sphere. (See Figure 2 for the definition of $\theta$ and $\phi$.) The $scf_e$ for the external source was calculated using Eq. (5) and determined to be 0.9870. The $scf_i$ for the internal source (40 W opal-bulb lamp, refer to 5.4) was calculated using Eq.(6) and determined to be 1.0003, which is almost negligible. To calculate $scf_i$, the relative luminous intensity distributions of the 40 W opal-bulb lamps were measured, with the cooperation of PTB(Physikalisch-Technische Bundesanstalt), Germany, using their goniophotometer.

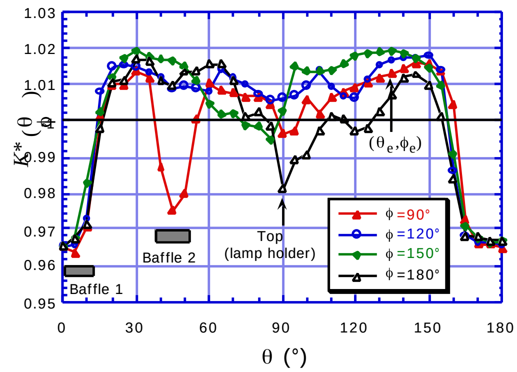


Figure 3 – The SRDF of the integrating sphere (upper hemisphere)

The incident angle dependence correction factor $\beta$ was measured according to the procedures described in 4.2. The same beam source (used for the SRDF measurement) was used. The correction factor $\beta$ in Eq.(8) was determined to be 0.9966, which was in approximate agreement with the data in reference [3].

Since the color temperatures of the external source (2856 K) and the internal sources (2730 K, refer to 5.4) were different, spectral mismatch corrections were made according to the procedures described in 4.3. The relative spectral throughput $T_s(\lambda)$ of the sphere was obtained using a spectroradiometer by taking the ratios of the spectral irradiance on the detector port of the sphere (in which a 500 W clear-bulb flux standard lamp was operated) and the spectral irradiance of the same lamp measured on the photometry bench. The relative spectral responsivity $R_s(\lambda)$ of the total integrating sphere system was then obtained using Eq.(10). Using Eq.(9), the spectral mismatch correction factors $ccf^*_i$ and $ccf^*_e$ were calculated to be 0.9982 and 1.0000, respectively.

## 5.3 Determination of the integrating sphere responsivity

A detector-based illuminance scale was introduced at NIST in 1991 [4]. The photometric responsivities of the eight standard photometers are calibrated annually against the spectral responsivity scale which is traceable to the NIST High Accuracy Cryogenic Radiometer (HACR). The uncertainty of the illuminance scale realization is 0.39 %.

The illuminance from the external source at the aperture plane was measured using a transfer photometer which was calibrated against the NIST standard photometers under illumination by the same frosted FEL lamp (used as the external source, operated at 2856 K), at a distance of ~3.5 m. The transfer photometer, with an opal diffuser (10 mm in diameter) in front, is equipped with a built-in temperature sensor which allow compensation for photometer temperature drift.

The illuminance distribution over the aperture area was measured by spatially scanning the transfer photometer to determine the average illuminance factor $k_a$ which is a ratio of the average illuminance $E_a$ to the illuminance on the aperture center $E_c$. Once $k_a$ is determined, only $E_c$ needs to be measured to obtain $E_a$.

The transfer photometer is attached to a holding plate which can be mounted interchangeably with the aperture.

[†] Throughout this paper, uncertainty is given as relative expanded uncertainty with coverage factor $k$=2, thus a two standard deviation estimate.

The position of the photometer on the holding plate is aligned, using an alignment telescope, so that the reference plane of the photometer and that of the limiting aperture coincide when they are mounted.

After measuring the illuminance $E_c$, the aperture is mounted, and the signal of the integrating sphere photometer $y_e$ is taken. The integrating sphere responsivity $R_s'$ is then determined by

$$R_s' = y_e \, ccf_e^* \, scf_e \, \beta \, / \, ( E_c \, k_a \, S ) \quad (11)$$

## 5.4 Calibration of primary standard lamps

A group of twelve 40 W opal-bulb incandescent lamps were calibrated to serve as the total luminous flux primary standards. At the same time, eight 60 W inside frosted incandescent lamps were also calibrated to serve as working standards. The calibrations of these 20 lamps were performed twice; first, a day before the determination of the sphere responsivity, and second, the same day immediately after the determination of the sphere responsivity. Self-absorption factors of all the 40 W and 60 W lamps, relative to the representative lamp, were also measured. The total luminous flux $\Phi_i$ of each lamp was assigned according to

$$\Phi_i = y_i \, ccf_i^* \, scf_i \, \alpha \, / \, R_s' \quad (12)$$

where $y_i$ is the detector signal for each lamp, and $\alpha$ is the self-absorption correction factor. The luminous flux values of each lamp reproduced to within ± 0.06 % in the two runs.

## 5.5 Comparison with a goniophotometer

In order to further verify the uncertainty of this integrating sphere method, the total luminous flux values of two of the 40 W opal-bulb lamps mentioned above were compared with values measured by a goniophotometer in PTB, Germany. The goniophotometer was calibrated against the NIST illuminance scale so that only the difference in the integrating sphere method and the goniophotometric method was compared, without influence of the difference in illuminance scale. This measurement was conducted in November 1993, and the luminous flux values of these two lamps were transferred to four other 40 W opal-bulb lamps when returned to NIST. The average difference, $(\Phi_s - \Phi_g) / \Phi_g$, of the luminous flux values of these 6 lamps measured by the sphere($\Phi_s$) and by the goniophotometer($\Phi_g$), was 0.20 % ± 0.17 % (two times the standard deviation of the mean).

## 5.6 Uncertainty budget

The uncertainty budget of the luminous flux scale realization is shown in Table 1. The overall uncertainty of the luminous flux scale realized on the 40 W opal-bulb lamps is estimated to be 0.53 %.

## 6. CONCLUSION

The integrating sphere method for realization of a luminous flux scale has been developed, and the NIST 1995 luminous flux scale has been established with a relative expanded uncertainty ($k$=2) of 0.53 %. The total luminous flux measured using the integrating sphere method agreed with the values obtained with a goniophotometer to within 0.2 %.

**Table 1.** Uncertainty budget for the NIST 1995 luminous flux scale

| Factor | Relative expanded uncertainty, $k$=2 [%] | |
|---|---|---|
| Uncertainty of the determination of $\Phi_e$ | | 0.41 |
| The NIST Illuminance scale realization | 0.39 | |
| Longterm drift of the std. photometers (2 months) | 0.03 | |
| Transfer to the transfer photometer | 0.07 | |
| Transfer photometer position alignment (±0.2 mm) | 0.06 | |
| Aperture alignment (difference of the two apertures) | 0.05 | |
| Aperture area | 0.03 | |
| Average illuminance factor $k_a$ | 0.03 | |
| Stray light | 0.04 | |
| Drift of the external source during calibration | 0.02 | |
| Uncertainty of the lamp luminous flux with respect to $\Phi_e$ | | 0.32 |
| Spatial correction factor $scf_i$ / $scf_e$ | 0.30 | |
| Incident angle dependence correction factor $\beta$ | 0.06 | |
| Spectral mismatch correction factor $ccf_i^*$ / $ccf_e^*$ | 0.03 | |
| Self-absorption correction factor $\alpha$ | 0.03 | |
| Random variation in the $R_s$ determination | 0.04 | |
| Detector linearity | 0.05 | |
| Reproducibility of the standard lamps | 0.06 | |
| Overall uncertainty of the NIST 1995 luminous flux scale | | 0.53 |

The magnitude of the new NIST luminous flux unit is 1.1 % larger than the previous unit, and hence, values measured with the new scale are 1.1 % smaller than previously reported. The new NIST luminous flux scale has been disseminated via NIST photometric calibration services since October, 1995.

The spatial correction technique using the SRDF is useful for conventional substitution measurements also. Using this technique, sources of known relative intensity distributions can be measured more accurately in an integrating sphere.

The integrating sphere method will also be useful in the total spectral radiant flux scale realization. Investigation of this application is underway at NIST.

## REFERENCES


[1] Ohno, Y.: Integrating sphere simulation: Application to total flux scale realization, *Appl. Opt.* **33**-13, pp. 2637-2647, 1994

[2] Ohno, Y.: New method for realizing total flux scale using an integrating sphere with an external source, *J. IES*, **24**-1, pp.106-115,1995

[3] Venable, W. H., Hsia, J. J., and Weidner, V. R. : Establishing a Scale of Directional-Hemispherical Reflectance Factor I: The Van den Akker Method, *J. R. NBS*, **82**-1: 29-55, 1977

[4] Ohno, Y., Cromer, C. L., Hardis, J. E., and Eppeldauer, G.: The detector-based candela scale and related photometric calibration procedures at NIST, *J. IES*, **23**-1, pp. 89-98, 1994



Yoshihiro Ohno
National Institute of Standards and Technology
A305, Bldg.220, Gaithersburg, MD 20899 USA



The author expresses sincere thanks to Dr. G. Sauter of PTB, Germany for his kind support in the measurements using the PTB goniophotometer and for fruitful discussions.